

# Uncertainty-based Detection of Adversarial Attacks in Semantic Segmentation

Kira Maag<sup>1</sup> and Asja Fischer<sup>1</sup>

<sup>1</sup>Ruhr University Bochum, Germany [{kira.maag, asja.fischer}@rub.de](mailto:{kira.maag, asja.fischer}@rub.de)

**Abstract.** State-of-the-art deep neural networks have proven to be highly powerful in a broad range of tasks, including semantic image segmentation. However, these networks are vulnerable against adversarial attacks, i.e., non-perceptible perturbations added to the input image causing incorrect predictions, which is hazardous in safety-critical applications like automated driving. Adversarial examples and defense strategies are well studied for the image classification task, while there has been limited research in the context of semantic segmentation. First works however show that the segmentation outcome can be severely distorted by adversarial attacks. In this work, we introduce an uncertainty-based method for the detection of adversarial attacks in semantic segmentation. We observe that uncertainty as for example captured by the entropy of the output distribution behaves differently on clean and perturbed images using this property to distinguish between the two cases. Our method works in a light-weight and post-processing manner, i.e., we do not modify the model or need knowledge of the process used for generating adversarial examples. In a thorough empirical analysis, we demonstrate the ability of our approach to detect perturbed images across multiple types of adversarial attacks.

## 1 Introduction

In recent years, deep neural networks (DNNs) have demonstrated outstanding performance and have proven to be highly expressive in a broad range of tasks, including semantic image segmentation [5, 30]. Semantic segmentation aims at segmenting objects in an image by assigning each pixel to a fixed and predefined set of semantic classes, providing comprehensive and precise information about the given scene. However, DNNs are vulnerable to *adversarial attacks* [3] which is very hazardous in safety-related applications like automated driving. Adversarial attacks are small perturbations added to the input image causing the DNN to perform incorrect predictions at test time. The perturbations are not perceptible to humans, making the detection of these examples very challenging, see for example Figure 1. This undesirable property of DNNs is a major security concern in real world applications. Hence, developing efficient strategies against adversarial attacks is of high importance. Such strategies can either increase the robustness of DNNs making it more difficult to generate adversarial examples (defense) or build on approaches to detect adversarial attacks (detection).

Adversarial attacks have attracted much attention, and numerous attacks as well as detection strategies have been proposed [15]. However, adversarial examples have not been analyzed extensively beyond standard image classification models, often using small datasets

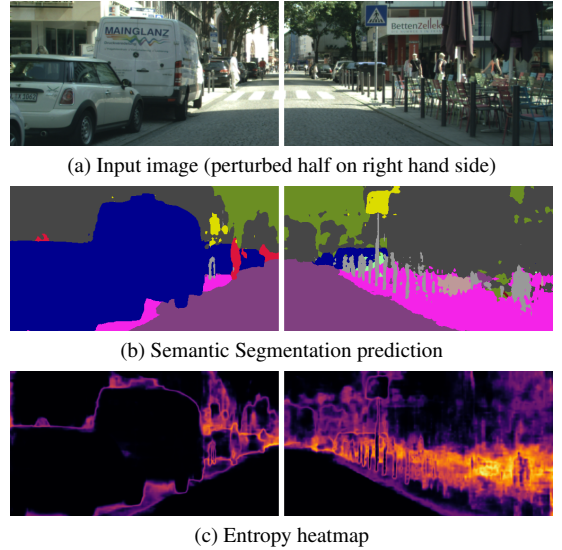


**Figure 1:** Semantic segmentation prediction and entropy heatmap for clean (left) and perturbed image (right) generated by a dynamic target attack for hiding pedestrians.

such as MNIST [19] or CIFAR10 [17]. The vulnerability of modern DNNs to attacks in more complex tasks like semantic segmentation in the context of real datasets from different domains has been rather poorly explored. The attacks which have been tested so far on semantic segmentation networks can be divided roughly into three categories. The first approaches transferred common attacks from image classification to semantic segmentation, i.e., pixel-wise classification [1, 13, 31]. Other works [8, 38] have presented attacks specifically designed for the task of semantic segmentation, either attacking the input in a way that leads to the prediction of some predefined and image-unrelated segmentation mask or the complete deletion of one segmentation class [25]. Such attacks are more difficult to detect than attacks that perturb each pixel independently. The third group of attacks creates rectangular patches smaller than the input size, which leads to erroneous prediction of the entire image [28, 29]. Defense methods aim to be robust against such attacks, i.e., to achieve high prediction accuracy even on perturbed images. For semantic segmentation tasks, defense approaches are often robust against only one type of attack [2, 16, 40]. In contrast, detection methods aim at classifying an input as clean or perturbed based on the output of the segmentation model [37].

In this paper, we present an uncertainty-based approach for detect-

ing several kinds of adversarial attacks on semantic image segmentation models. Uncertainty information has already been exploited for the detection of adversarial attacks on classification DNNs, but has not been investigated in the context of segmentation so far. In [11], an approximation to Bayesian inference (Monte-Carlo Dropout), which is widely employed to estimate model uncertainty, is considered for the detection of adversarial attacks. The gradient-based approach introduced in [26] generates salient features which are used to train a detector. While both methods require access to the inside of the model, our approach can be applied as a post-processing step using only information of the network output. We construct features per image based on the uncertainty information provided by the DNN such as entropy. In Figure 1 (c), the entropy heatmaps for a clean (left) and a perturbed image (right) are shown, indicating high uncertainties in the attacked regions, motivating the use of uncertainty information to separate clean and perturbed images. On the one hand, these features for clean and perturbed inputs are fed into a one-class support vector machine that performs unsupervised novelty detection [36]. On the other hand, we train a logistic regression model with clean and perturbed data for classification. The perturbed data used during training is generated by only one kind of adversarial attack method, while the detector is applied to identify adversarial examples of other methods. Note, for the image classification task, an ensemble of detectors [24] and a multi-layer perceptron [42] are considered to decide between clean and attacked images achieving high results. For semantic segmentation, post-processing classification models are used for false positive detection [22, 21] and out-of-distribution segmentation [20], although not for adversarial examples. Our method neither modifies the semantic segmentation model nor requires knowledge of the process for generating adversarial examples. We only assume that our post-processing model is kept private while the attacker may have full access to the semantic segmentation model. An overview of our approach is shown in Figure 2.

In our tests, we employ state-of-the-art semantic segmentation networks [5, 30] applied to the Cityscapes [9] as well as Pascal VOC2012 dataset [10] demonstrating our adversarial attack detection performance. To this end, we consider different types of attackers, from pixel-level attacks designed for image classification [12, 18] to pixel-wise attacks developed for semantic segmentation [25], and patch-based ones [29]. The source code of our method is publicly available at <https://github.com/kmaag/Adversarial-Attack-Detection-Uncertainty>. Our contributions are summarized as follows:

- We introduce a new uncertainty-based method for the detection of adversarial attacks for the semantic image segmentation task. To this end, we feed a set of uncertainty-based features into a supervised as well as unsupervised classification model. Our approach serves as a light-weight post-processing step, i.e., we do not modify the model or need knowledge of the process for generating adversarial examples.
- For the first time, we present a detection method that was not designed for a specific adversarial attack, rather has a high detection capability across multiple types. We achieve averaged detection accuracy values of up to 100% for different network architectures and datasets.

The paper is structured as follows. In section 2, we discuss the related work on defense and detection methods for adversarial attacks applied to semantic segmentation models. The different adversarial attacks are shown in section 3. In section 4, we introduce our detection method. The numerical results are presented in section 5, fol-

lowed by a conclusion in section 6.

## 2 Related Work

In this section, we discuss the related works on defense and detection methods for the semantic segmentation task. Defense methods aim to achieve high prediction accuracy even on perturbed images, while detection methods classify the model input as clean or attacked image. A dynamic divide-and-conquer strategy [39] and multi-task training [16], which extends supervised semantic segmentation by a self-supervised monocular depth estimation using unlabeled videos, are considered as adversarial training approaches enhancing the robustness of the networks. Another kind of defense strategy is input denoising to remove the perturbation from the input without the necessity to re-train the model. In [3] image quilting and the non-local means algorithm are presented as input transformation techniques. To denoise the perturbation and restore the original image, a denoise autoencoder is used in [6]. The demasked smoothing technique, introduced in [40], reconstructs masked regions of each image based on the available information with an inpainting model defending against patch attacks. Another possibility to increase the robustness of the model is during inference. In [2] is shown how mean-field inference and multi-scale processing naturally form an adversarial defense. The non-local context encoder proposed in [14] models spatial dependencies and encodes global contexts for strengthening feature activations. From all pyramid features multi-scale information is fused to refine the prediction and create segmentation. The presented works up to now are defense methods improving the robustness of the model. To the best of our knowledge so far only one work focuses on detecting adversarial attacks on segmentation models, i.e., the patch-wise spatial consistency check is introduced in [37] to detect adversarial examples.

The described defense approaches are created for and tested only on a specific type of attack. The problem is that you assume a high model robustness, however, the defense method may perform poorly on new unseen attacks and does not provide a statement about this insecurity. Therefore, we present a detection method which shows strong results over several types of adversarial attacks. The presented detection approach [37] is only tested on perturbed images attacked in such a way that a selected image is predicted. The spatial consistency check randomly selects overlapping patches to obtain pixel-wise confidence vectors. In contrast, our method use only information of the network output from one inference and not from (computationally expensive) multiple runs of the network. For these reasons, the detection approach from [37] cannot be considered as a suitable baseline.

## 3 Adversarial Attacks

For the generation of adversarial examples, we distinguish between *white* and *black box* attacks. White box attacks are created based on information of the victim model, i.e., the adversarial has access to the full model, including its parameters, and knows the loss function used for training. In contrast, black box attackers have zero knowledge about the victim model. The idea behind these type of attacks is transferability, i.e., an adversarial example generated from another model works well with the victim one. The attacks described in the following belong to the white box setting and were proposed to attack semantic segmentation models.

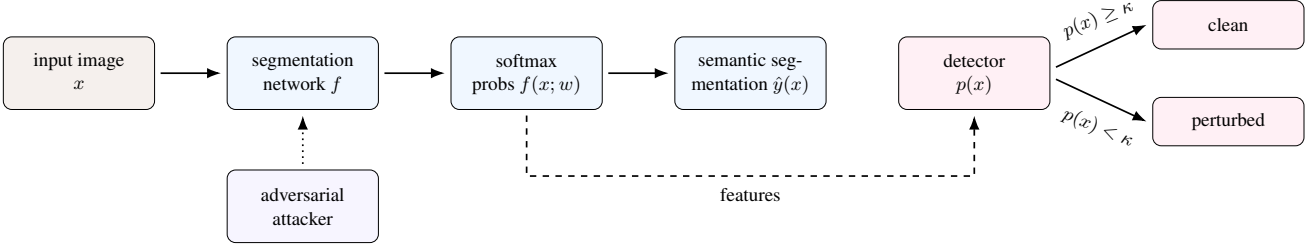


**Figure 2:** Schematic illustration of our detection method. The adversarial attacker can have full access to the semantic segmentation model. Information from the network output is extracted to construct the features which serve as input to the detector model classifying between clean and perturbed images.

**Attacks on Pixel-wise Classification** The attacks described in this paragraph were originally developed for image classification and were (in a modified version) applied to semantic segmentation. For semantic segmentation, given an image  $x$  a neural network with parameters  $w$  provides pixel-wise probability distributions  $f(x; w)_{ij}$  over a label space  $C = \{y_1, \dots, y_c\}$  per spatial dimension  $(i, j)$ . The single-step untargeted *fast gradient sign method* (FGSM, [12]) creates adversarial examples by adding perturbations to the pixels of an image  $x$  with label  $y$  that leads to an increase of the loss  $L$  (here cross entropy), that is

$$x_{ij}^{adv} = x_{ij} + \varepsilon \cdot \text{sign}(\nabla_x L_{ij}(f(x; w)_{ij}, y_{ij})) , \quad (1)$$

where  $\varepsilon$  is the magnitude of perturbation. The single-step targeted attack with target label  $y_{tl}$  instead decreases the loss for the target label and is given by

$$x_{ij}^{adv} = x_{ij} - \varepsilon \cdot \text{sign}(\nabla_x L_{ij}(f(x; w)_{ij}, y_{ij}^{tl})) . \quad (2)$$

Following the convention, the least likely class predicted by the model is chosen as target class. This attack is extended in [18] in an iterative manner (I-FGSM) to increase the perturbation strength

$$x_{ij,t+1}^{adv} = \text{clip}_{x,\varepsilon}(x_{ij,t}^{adv} + \alpha \cdot \text{sign}(\nabla_{x_t^{adv}} L_{ij}(f(x_t^{adv}; w)_{ij}, y_{ij}))) \quad (3)$$

with  $x_0^{adv} = x$ , step size  $\alpha$ , and a clip function ensuring that  $x_t^{adv} \in [x - \varepsilon, x + \varepsilon]$ . The targeted case (see Equation 2) can be formulated analogously. Based on these attacks, further methods for pixel-wise perturbations in the classification context have been proposed such as projected gradient descent (PGD) [23, 4] and DeepFool [27]. Some of these approaches have been further developed and adapted for the semantic segmentation task [1, 13, 31].

**Stationary Segmentation Mask Attacks** Another type of attacks are so called *stationary segmentation mask methods* (SSMM) where the pixels of a whole image are iteratively attacked until most of the pixels have been mis-classified into the target class [8, 38]. For each spatial dimension  $(i, j) \in \mathcal{I}$ , the loss function per image  $x$  is given by

$$L(f(x; w), y) = \frac{1}{|\mathcal{I}|} \sum_{(i, j) \in \mathcal{I}} L_{ij}(f(x; w)_{ij}, y_{ij}) . \quad (4)$$

In [25], the universal perturbation is introduced to achieve real-time performance for the attack at test time. To this end, training inputs  $D^{\text{train}} = \{x^{(k)}, y^{(k),\text{target}}\}_{k=1}^m$  are generated where  $y^{(k),\text{target}}$  defines a fixed target segmentation. The universal noise in iteration  $t + 1$  is computed by

$$\xi_{t+1} = \text{clip}_{\varepsilon}(\xi_t - \alpha \cdot \text{sign}(\frac{1}{m} \sum_{k=1}^m \nabla_x L(f(x^{(k)} + \xi_t; w), y^{(k),\text{target}}))) \quad (5)$$

with  $\xi_0 = 0$ . The loss of pixels which are predicted as belonging to the desired target class with a confidence above a threshold  $\tau$  are set to 0. At test time, this noise is added to the input image and does not require multiple calculations of the backward pass.

The *dynamic nearest neighbor method* (DNNM) presented in [25] aims to keep the network's segmentation unchanged but to remove a desired target class. Let  $o$  be the object class being deleted and  $\hat{y}(x)_{ij} = \arg \max_{y \in C} f(x; w)_{ij}$  the predicted class, then  $\mathcal{I}_o = \{(i, j) | \hat{y}(x)_{ij} = o\}$  and  $\mathcal{I}_{\bar{o}} = \mathcal{I} \setminus \mathcal{I}_o$ . The target label is chosen by  $y_{ij}^{\text{target}} = \hat{y}(x)_{i'j'}$  with  $\arg \min_{(i', j') \in \mathcal{I}_{\bar{o}}} (i' - i)^2 + (j' - j)^2$  for all  $(i, j) \in \mathcal{I}_o$  and  $y_{ij}^{\text{target}} = \hat{y}(x)_{ij}$  for all  $(i, j) \in \mathcal{I}_{\bar{o}}$ . Since the loss function described in Equation 4 weights all pixels equally though both objectives, i.e., hiding a object class and being unobtrusive, are not necessarily equally important, a modified version of the loss function with weighting parameter  $\omega$  is given by

$$L^{\omega}(f(x; w), y) = \frac{1}{|\mathcal{I}|} (\omega \sum_{(i, j) \in \mathcal{I}_o} L_{ij}(f(x; w)_{ij}, y_{ij}^{\text{target}}) + (1 - \omega) \sum_{(i, j) \in \mathcal{I}_{\bar{o}}} L_{ij}(f(x; w)_{ij}, y_{ij}^{\text{target}})) . \quad (6)$$

Note, the universal perturbation can also be computed for the DNNM.

**Patch-based Attacks** The idea behind *patch attacks* is that perturbing a small region of the image causes prediction errors in a much larger region [28]. In [29], the *expectation over transformation* (EOT)-based patch attack is introduced to create robust adversarial examples, i.e., individual adversarial examples that are at the same time adversarial over a range of transformations. Transformations occurring in the real world are for instance angle and viewpoint changes. These perturbations are modeled within the optimization procedure and an extension of the pixel-wise cross entropy loss is additionally presented in [29] to enable crafting strong patches for the semantic segmentation setting.

## 4 Detection Method

Our method does not alter the semantic segmentation model, nor does it require knowledge of the adversarial example generation process. While the attacker may have full access to the semantic segmentation model, we only assume that our post-processing model is kept secret or not attacked. Our approach can be applied as a post-processing step using only information of the network output. In Figure 2 an overview of our approach is given.

The degree of uncertainty in a semantic segmentation prediction is

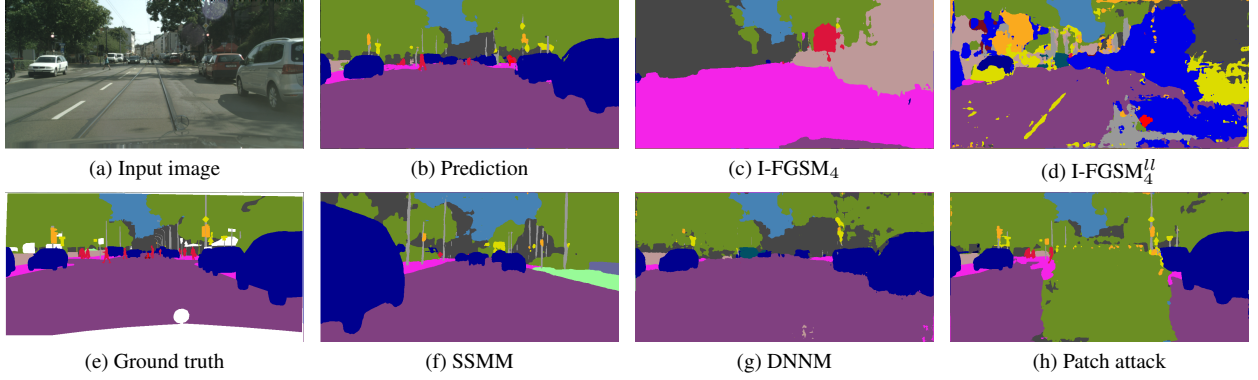


**Figure 3:** Input image (a) with corresponding ground truth (e). Semantic segmentation prediction for clean (b) and perturbed image generated by an untargeted (c) and a targeted FGSM attack (d) as well as by a SSMM (f), a DNNM (g) and a patch attack (h).

quantified by pixel-wise dispersion measures like the entropy

$$E(x)_{ij} = - \sum_{y \in \mathcal{C}} f(x; w)_{ij} \log f(x; w)_{ij} , \quad (7)$$

the variation ratio

$$V(x)_{ij} = 1 - \max_{y \in \mathcal{C}} f(x; w)_{ij} , \quad (8)$$

or the probability margin

$$M(x)_{ij} = V(x)_{ij} + \max_{y \in \mathcal{C} \setminus \{\hat{y}(x)_{ij}\}} f(x; w)_{ij} . \quad (9)$$

The entropy heatmaps for a clean (left) and a perturbed image (right) are shown in Figure 1 (c) indicating that higher uncertainties occur in the attacked regions which motivates the use of uncertainty information to separate clean and perturbed data. To obtain uncertainty features per image from these pixel-wise dispersion measures, we aggregate them over a whole image by calculating the averages

$$\bar{D} = \frac{1}{|\mathcal{I}|} \sum_{(i,j) \in \mathcal{I}} D(x)_{ij} , \quad (10)$$

where  $D \in \{E, V, M\}$ . Moreover, we obtain mean class probabilities for each class  $y \in \{1, \dots, C\}$

$$P(y|x) = \frac{1}{|\mathcal{I}|} \sum_{(i,j) \in \mathcal{I}} f(x; w)_{ij} . \quad (11)$$

Note, these features can be computed without the knowledge of the ground truth label.

We compute these image-wise features for a set of benign (and adversarially changed) images, which can then be used to train classification models providing per image a probability  $p(x)$  of being clean (and not perturbed). We classify  $x$  as perturbed if  $p(x) < \kappa$  and as clean if  $p(x) \geq \kappa$ , where  $\kappa$  is a predefined detection threshold. We apply different ways to construct such a classifier. First, we consider the one-class support vector machine (OCSVM, [33]) as detection model. The OCSVM performs unsupervised novelty detection using clean (and if present perturbed) data to learn a small region capturing the clean data points projected into a higher dimensional feature space. The result is a binary function that classifies points mapped into the region as data points and observations mapped outside this region as anomaly. Since detecting outliers in high-dimensional data (without assumptions about the distribution of the underlying data)

is very challenging, we assume that the data is Gaussian and study an approach for detecting outliers in a Gaussian distributed dataset learning an ellipse [32].

Second, we consider the supervised logistic regression (LASSO [34]) as classification model trained on clean and perturbed images. Importantly, we do not require knowledge of the adversarial example generation process used by the attacker, instead we use attacked data generated by any (other) adversarial attack (cross-attack). Note, applying our detection method is light-weight, i.e., the feature computation is inexpensive and classification models are trained in advance so that only one inference run is added after semantic segmentation inference.

## 5 Experiments

First, we present the experimental setting and then evaluate our adversarial detection method.

### 5.1 Experimental Setting

**Datasets** We perform our tests on the Cityscapes [9] dataset for semantic segmentation in street and on the Pascal VOC2012 [10] (shorthand VOC) dataset of visual object classes in realistic scenes. The Cityscapes dataset consists of 2,975 training and 500 validation images of dense urban traffic in 18 and 3 different German towns, respectively. The VOC dataset contains 1,464 training and 1,449 validation images with annotations for the various objects of categories person, animal, vehicle and indoor.

**Segmentation Networks** We consider the state-of-the-art DeepLabv3+ network [5] with Xception65 backbone [7]. Trained on Cityscapes, we achieve a mean intersection over union (mIoU) value of 78.93 on the validation set and trained on VOC, a validation mIoU value of 88.39. Moreover, we use the BiSeNet [41] trained on Cityscapes obtaining a validation mIoU of 70.32. We consider also two real-time models for the Cityscapes dataset, the DDRNet [30] achieving 77.8 mIoU and the HRNet [35] with 70.5 mIoU.

**Adversarial Attacks** In many defense methods in semantic segmentation, the adapted FGSM and I-FGSM attack are employed [2, 3, 14, 16, 39]. Thus, we study both attacks in our experiments with the parameter setting presented in [18]. The magnitude of noise

is given by  $\varepsilon = \{4, 8, 16\}$ , the step size by  $\alpha = 1$ , and the number of iterations is computed as  $n = \min\{\varepsilon + 4, 1.25\varepsilon\}$ . We denote by  $\text{FGSM}_\varepsilon^\#$  and  $\text{I-FGSM}_\varepsilon^\#$ ,  $\# \in \{\_, ll\}$ , the (iterative) attack where the superscript discriminates between untargeted and targeted (least likely). For the re-implementation of SSMM and DNNM [25], we use the parameters  $\varepsilon = 0.1 \cdot 255$ ,  $\alpha = 0.01 \cdot 255$ ,  $n = 60$  and  $\tau = 0.75$ . For SSMM, the target image is chosen randomly for both datasets and for DNNM, the class person is to be deleted for the Cityscapes dataset. For the VOC dataset, the DNNM attack makes no sense, since on the input images often only one object or several objects of the same class are contained. For our experiments, we use a model zoo<sup>1</sup> where we add the implementations of the adversarial attacks FGSM, I-FGSM, SSMM and DNNM. As we also use the pre-trained networks provided in the repository, we run experiments for the Cityscapes dataset on both models, DeepLabv3+ and HRNet, and for VOC on the DeepLabv3+ network.

For the patch attack introduced in [29], we use the provided code<sup>2</sup> with default parameters and consider two different segmentation models, BiSeNet and DDRNet, applied to the one tested real world dataset (Cityscapes). Since we use the cross-attack procedure for our detection model (logistic regression), i.e., we train the classifier on clean and perturbed data attacked by an attack other than the patch, we use the data obtained from the DeepLabv3+ to train the detector and test on the DDRNet. For the HRNet and the BiSeNet we proceed analogously, since in each case the prediction performance (in terms of mIoU) of both networks is similar.

As the Cityscapes dataset provides high-resolution images ( $1024 \times 2048$  pixels) which require a great amount of memory to run a full backward pass for the computation of adversarial samples, we re-scale image size for this dataset to  $512 \times 1024$  when evaluating. In Figure 3, a selection of these attacks is shown for the Cityscapes dataset and the DeepLabv3+ network (or DDRNet for the patch attack).

**Evaluation Metrics** Our detection model provides per image a probability  $p(x)$  of being clean (and not perturbed). We threshold on this probability with 40 different values  $\kappa \in [0, 1]$ . Firstly, the detection accuracy is defined as the proportion of clean images that are predicted correctly with respect to non-detected clean images and detected perturbed images. Note, this metric depends on a threshold  $\kappa$ . The averaged detection accuracy (ADA( $\kappa$ )) calculates the average over the detection accuracy for clean and perturbed images. The optimal ADA score is obtained by  $\text{ADA}^* = \max_{\kappa \in [0, 1]} \text{ADA}(\kappa)$ . Secondly, we compute the area under the receiver operating characteristic curve (AUROC) by varying the decision threshold to obtain a threshold independent metric. Lastly, we consider the true positive rate while fixing the false positive rate on clean images to 5% (TPR<sub>5%</sub>).

## 5.2 Numerical Results

In the following, we study the attack success performance and evaluate our adversarial attack detection performance.

**Attack Performance** In order to access the performance of the attackers, we consider the attack pixel success rate (APSR) [31] de-

fined by

$$\text{APSR} = \frac{1}{|\mathcal{I}|} \sum_{(i,j) \in \mathcal{I}} \arg \max_{y \in \mathcal{C}} f(x^{adv}; w)_{ij} \neq y_{ij} . \quad (12)$$

Note, this metric is the opposite of the accuracy, as it focuses on falsely (and not correct) predicted pixels. If we replace  $x^{adv}$  in Equation 12 by the input image  $x$ , we obtain a measure how well the semantic segmentation model performs on clean data. The values for this measure for the different networks and both datasets are given in Table 1. As expected, we observe small APSR scores: all values are below 6.84%.

**Table 1:** APSR results for the semantic segmentation predictions on clean data of the different network architectures and both datasets.

	DeepLabv3+	DDRNet	HRNet	BiSeNet
Cityscapes	6.84	4.00	5.48	5.26
VOC	2.92	-	-	-

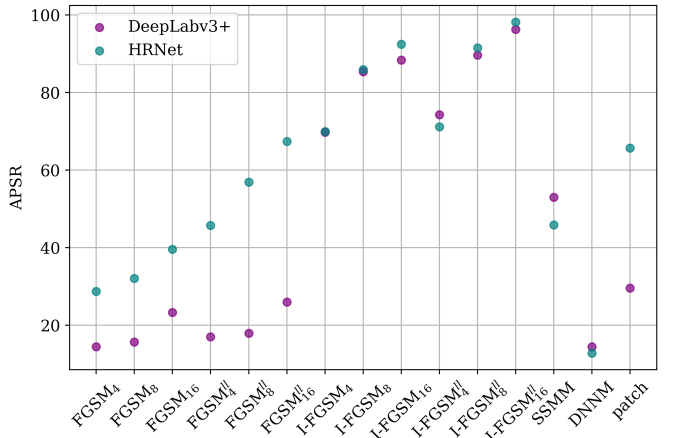


**Figure 4:** APSR results for the Cityscapes dataset and both networks perturbed by different attacks.

The APSR results for various attacks on the Cityscapes dataset are shown in Figure 4. For all variations of the FGSM attack (untargeted vs. targeted, non-iterative vs. iterative) the APSR increases with larger magnitude of the noise. The I-FGSM outperforms the FGSM due to the iterative procedure of individual perturbation steps. For the SSMM attack, a randomly chosen image from the dataset is predicted. In Figure 3, the prediction of the clean and the perturbed image reveal similarities in some areas, such as the street or the sky, which reflects the nature of street scenes. For this reason, the values range around 50%. For the DNNM attack, the APSR scores are comparatively small since most parts of the images are not perturbed, only one class is to be deleted. We observe that the performance of the patch attack has more or less impact depending on the model. Comparing the two models, we find that DeepLabv3+ is more robust against adversarial attacks, as the APSR values are mostly smaller than those of the HRNet network. A selection of qualitative results is shown in Appendix A.

The results for the VOC dataset given in Table 2 are qualitatively similar to the findings for the Cityscapes dataset. However, the outcome for the (targeted as well as untargeted) non-iterative FGSM attack differs, i.e., the APSR scores are not increasing with higher noise but stay at similar values. This observation is confirmed in the

<sup>1</sup> <https://github.com/LikeLy-Journey/SegmenTron>

<sup>2</sup> <https://github.com/retis-ai/SemSegAdvPatch/>

**Table 2:** APSR results for the VOC dataset and the DeepLabv3+ network perturbed by different attacks.

FGSM <sub>4</sub>	FGSM <sub>8</sub>	FGSM <sub>16</sub>	FGSM <sub>4</sub> <sup>II</sup>	FGSM <sub>8</sub> <sup>II</sup>	FGSM <sub>16</sub> <sup>II</sup>	I-FGSM <sub>4</sub>	I-FGSM <sub>8</sub>	I-FGSM <sub>16</sub>	I-FGSM <sub>4</sub> <sup>II</sup>	I-FGSM <sub>8</sub> <sup>II</sup>	I-FGSM <sub>16</sub> <sup>II</sup>	SSMM
17.81	17.93	16.67	19.68	19.66	17.65	56.73	74.94	80.98	64.30	82.51	91.68	62.99

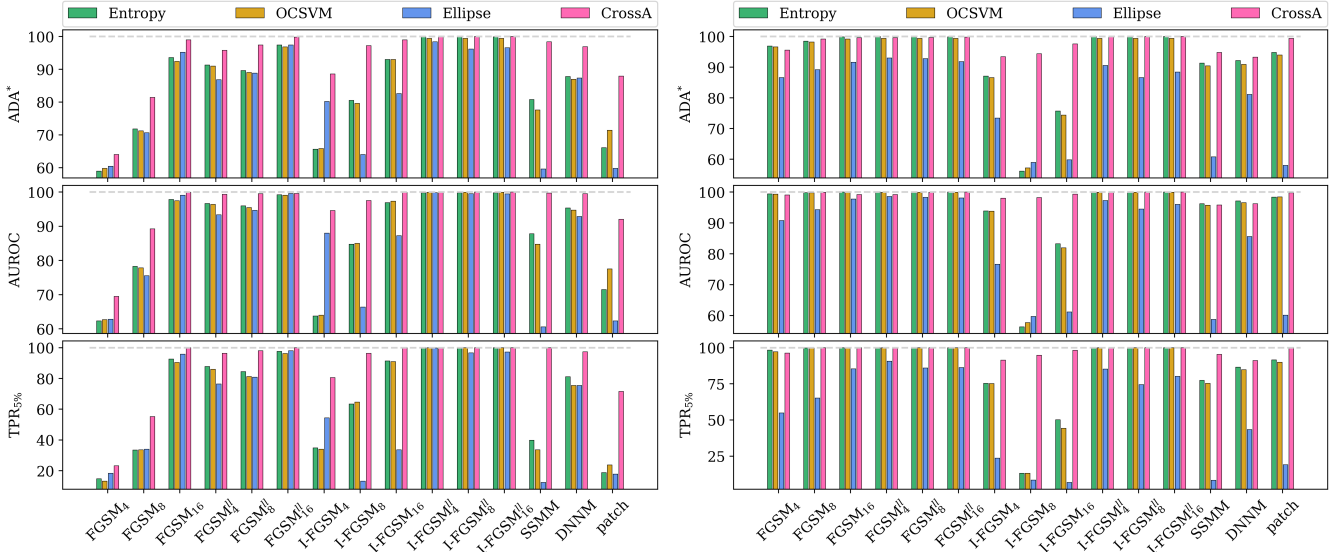


**Figure 5:** Detection performance results for the Cityscapes dataset as well as the DeepLabv3+ (left) and the HRNet (right).

**Table 3:** Detection performance results for the VOC dataset and the DeepLabv3+ network.

ADA* ↑	FGSM <sub>4</sub>	FGSM <sub>8</sub>	FGSM <sub>16</sub>	FGSM <sub>4</sub> <sup>II</sup>	FGSM <sub>8</sub> <sup>II</sup>	FGSM <sub>16</sub> <sup>II</sup>	I-FGSM <sub>4</sub>	I-FGSM <sub>8</sub>	I-FGSM <sub>16</sub>	I-FGSM <sub>4</sub> <sup>II</sup>	I-FGSM <sub>8</sub> <sup>II</sup>	I-FGSM <sub>16</sub> <sup>II</sup>	SSMM
Entropy	65.94	66.87	67.60	76.54	77.16	76.71	65.84	51.86	63.39	95.76	93.58	94.38	<b>93.86</b>
OCSVM	66.49	67.12	67.81	75.95	76.57	76.29	66.29	52.14	63.87	95.27	93.06	93.62	93.48
Ellipse	66.15	67.05	67.46	75.60	76.85	76.09	64.63	57.80	56.69	94.72	92.93	94.24	78.50
CrossA	<b>69.46</b>	<b>70.36</b>	<b>70.91</b>	<b>84.85</b>	<b>84.92</b>	<b>83.61</b>	<b>71.19</b>	<b>82.78</b>	<b>88.92</b>	<b>98.38</b>	<b>99.14</b>	<b>99.69</b>	93.69
AUROC ↑	FGSM <sub>4</sub>	FGSM <sub>8</sub>	FGSM <sub>16</sub>	FGSM <sub>4</sub> <sup>II</sup>	FGSM <sub>8</sub> <sup>II</sup>	FGSM <sub>16</sub> <sup>II</sup>	I-FGSM <sub>4</sub>	I-FGSM <sub>8</sub>	I-FGSM <sub>16</sub>	I-FGSM <sub>4</sub> <sup>II</sup>	I-FGSM <sub>8</sub> <sup>II</sup>	I-FGSM <sub>16</sub> <sup>II</sup>	SSMM
Entropy	71.82	73.10	74.05	83.93	84.55	83.61	69.69	49.50	64.66	<b>99.19</b>	97.64	96.71	96.34
OCSVM	72.10	73.25	74.10	83.30	84.07	83.14	69.84	49.24	65.83	99.01	97.27	96.36	96.29
Ellipse	69.08	70.21	70.97	82.25	82.74	81.77	68.57	56.22	46.58	99.01	98.18	98.16	83.71
CrossA	<b>74.16</b>	<b>75.94</b>	<b>77.27</b>	<b>91.52</b>	<b>91.55</b>	<b>90.49</b>	<b>74.69</b>	<b>86.19</b>	<b>93.37</b>	99.08	<b>99.94</b>	<b>99.91</b>	<b>96.46</b>
TPR <sub>5%</sub> ↑	FGSM <sub>4</sub>	FGSM <sub>8</sub>	FGSM <sub>16</sub>	FGSM <sub>4</sub> <sup>II</sup>	FGSM <sub>8</sub> <sup>II</sup>	FGSM <sub>16</sub> <sup>II</sup>	I-FGSM <sub>4</sub>	I-FGSM <sub>8</sub>	I-FGSM <sub>16</sub>	I-FGSM <sub>4</sub> <sup>II</sup>	I-FGSM <sub>8</sub> <sup>II</sup>	I-FGSM <sub>16</sub> <sup>II</sup>	SSMM
Entropy	19.46	22.50	24.43	47.62	50.03	46.65	16.77	6.21	12.91	95.72	91.30	92.13	76.67
OCSVM	21.46	22.43	26.50	48.03	48.45	47.90	17.18	6.42	27.47	95.45	90.61	91.17	79.92
Ellipse	21.33	22.15	22.50	48.10	48.38	47.69	15.94	6.63	2.48	94.82	90.27	91.79	31.82
CrossA	<b>27.26</b>	<b>32.09</b>	<b>32.23</b>	<b>68.74</b>	<b>69.01</b>	<b>64.11</b>	<b>42.51</b>	<b>69.22</b>	<b>74.05</b>	<b>98.76</b>	<b>100.00</b>	<b>100.00</b>	<b>84.89</b>

sample images in the Appendix A which show very little variation over the various magnitudes of noise.

In summary, for both datasets and the different network architectures, most attacks achieve high APSR values and greatly alter the prediction. Thus, the detection of such attacks is extremely important.

**Evaluation of our Detection Method** The defense approaches described in section 2 are created for and tested only on a specific type of attacks. The sole presented detection approach [37] is only tested on stationary segmentation mask methods and is computationally expensive due to the requirement of multiple runs of the network. For this reason, neither this detection approach nor the defense methods can be considered as suitable baselines. Therefore, we consider the mean entropy as simple baseline in our experiments, which provides an uncertainty score per image comparable with the probability given by our detector.

The detection results for the Cityscapes dataset are shown in Figure

5 and for the VOC dataset in Table 3. We denote the ordinary one-class support vector machine by *OCSVM*, learned ellipse (under assumption that the data is Gaussian distributed) by *Ellipse* and the logistic regression model by *CrossA*. Note, the training of these models is light-weight and no knowledge of the process for generating adversarial examples is needed. We observe comparatively weaker detection performance results for smaller magnitudes of noise for the different FGSM attacks as smaller perturbations are more difficult to detect. The methods perform quit differently for the I-FGSM attack which is harder to detect since the prediction results consist only of a few classes (see Figure 3 (c)) with often low uncertainty for large connected components. However, CrossA performs very well. A similar behavior is observed for the SSMM and the patch attack. Most interesting are the high detection results by CrossA, up to 96.89% ADA\* values, for the DNNM attack as the perturbation targets only a few pixels and is therefore difficult to detect. To sum up, we outperform the entropy baseline and CrossA is by far the strongest detector achieving ADA\* values of up to 100%.

## 6 Conclusion

In this work, we introduced a new uncertainty-based method for the detection of adversarial attacks for the semantic image segmentation task. While adversarial examples are well studied for the image classification task, there has been limited research on adversarial attacks on semantic segmentation. We presented the first detection approach that was not designed for a specific adversarial attack, but has a high detection capability across multiple types. We observed that uncertainty information such as entropy behaves differently on clean and perturbed images and used this property to distinguish between the two cases. Our method works in a light-weight and post-processing manner, i.e., we do not modify the model nor need knowledge of the process used by the attacker for generating adversarial examples. We achieve averaged detection accuracy values of up to 100% for different network architectures and datasets.

## Acknowledgements

This work is supported by the Ministry of Culture and Science of the German state of North Rhine-Westphalia as part of the KI-Starter research funding program.

## References

- [1] Shashank Agnihotri and Margret Keuper. Cospgd: a unified white-box adversarial attack for pixel-wise prediction tasks, 2023.
- [2] Anurag Arnab, Ondrej Miksik, and Philip Torr, ‘On the robustness of semantic segmentation models to adversarial attacks’, in *IEEE/CVF Conference on Computer Vision and Pattern Recognition (CVPR)*, (2018).
- [3] Andreas Bar, Jonas Lohdefink, Nikhil Kapoor, Serin Varghese, Fabian Huger, Peter Schlicht, and Tim Fingscheidt, ‘The vulnerability of semantic segmentation networks to adversarial attacks in autonomous driving: Enhancing extensive environment sensing’, *IEEE Signal Processing Magazine*, (2021).
- [4] Oliver Bryniarski, Nabeel Hingun, Pedro Pachuca, Vincent Wang, and Nicholas Carlini, ‘Evading adversarial example detection defenses with orthogonal projected gradient descent’, in *International Conference on Learning Representations (ICLR)*, (2022).
- [5] Liang-Chieh Chen, Yukun Zhu, George Papandreou, Florian Schroff, and Hartwig Adam, ‘Encoder-decoder with atrous separable convolution for semantic image segmentation’, in *European Conference on Computer Vision (ECCV)*, (2018).
- [6] Seungju Cho, Tae Joon Jun, Byungsoo Oh, and Daeyoung Kim, ‘Dapas : Denoising autoencoder to prevent adversarial attack in semantic segmentation’, in *International Joint Conference on Neural Network (IJCNN)*, (2020).
- [7] François Chollet, ‘Xception: Deep learning with depthwise separable convolutions’, *IEEE Conference on Computer Vision and Pattern Recognition (CVPR)*, (2017).
- [8] Moustapha Cisse, Yossi Adi, Natalia Neverova, and Joseph Keshet, ‘Houdini: Fooling deep structured prediction models’, in *Conference on Neural Information Processing Systems (NeurIPS)*, (2017).
- [9] Marius Cordts, Mohamed Omran, Sebastian Ramos, Timo Rehfeld, Markus Enzweiler, Rodrigo Benenson, Uwe Franke, Stefan Roth, and Bernt Schiele, ‘The cityscapes dataset for semantic urban scene understanding’, in *IEEE Conference on Computer Vision and Pattern Recognition (CVPR)*, (2016).
- [10] Mark Everingham, Luc Van Gool, Chris K. I. Williams, John Winn, and Andrew Zisserman. The PASCAL Visual Object Classes Challenge 2012 (VOC2012) Results. <http://www.pascal-network.org/challenges/VOC/voc2012/workshop/index.html>.
- [11] Reuben Feinman, Ryan R. Curtin, Saurabh Shintre, and Andrew B. Gardner. Detecting adversarial samples from artifacts, 2017.
- [12] Ian J. Goodfellow, Jonathon Shlens, and Christian Szegedy, ‘Explaining and harnessing adversarial examples’, in *International Conference on Learning Representations (ICLR)*, eds., Yoshua Bengio and Yann LeCun, (2015).
- [13] Jindong Gu, Hengshuang Zhao, Volker Tresp, and Philip Torr, ‘Segpgd: An effective and efficient adversarial attack for evaluating and boosting segmentation robustness’, in *European Conference on Computer Vision (ECCV)*, (2022).
- [14] Xiang He, Sibei Yang, Guanbin Li, Haofeng Li, Huiyou Chang, and Yizhou Yu, ‘Non-local context encoder: Robust biomedical image segmentation against adversarial attacks’, in *AAAI Conference on Artificial Intelligence*, (2019).
- [15] Samer Y. Khamaiseh, Derek Bagagem, Abdullah Al-Alaj, Mathew Mancino, and Hakam W. Alomari, ‘Adversarial deep learning: A survey on adversarial attacks and defense mechanisms on image classification’, *IEEE Access*, (2022).
- [16] Marvin Klingner, Andreas Bär, and Tim Fingscheidt, ‘Improved noise and attack robustness for semantic segmentation by using multi-task training with self-supervised depth estimation’, in *IEEE/CVF Conference on Computer Vision and Pattern Recognition Workshop (CVPRW)*, (2020).
- [17] Alex Krizhevsky, ‘Learning multiple layers of features from tiny images’, (2009).
- [18] Alexey Kurakin, Ian J. Goodfellow, and Samy Bengio, ‘Adversarial machine learning at scale’, in *International Conference on Learning Representations (ICLR)*, (2017).
- [19] Yann LeCun and Corinna Cortes, ‘MNIST handwritten digit database’, (2010).
- [20] Kira Maag, Robin Chan, Svenja Uhlemeyer, Kamil Kowol, and Hanno Gottschalk, ‘Two video data sets for tracking and retrieval of out of distribution objects’, in *Asian Conference on Computer Vision (ACCV)*, pp. 3776–3794, (2022).
- [21] Kira Maag and Matthias Rottmann, ‘False negative reduction in semantic segmentation under domain shift using depth estimation’, in *International Joint Conference on Computer Vision, Imaging and Computer Graphics Theory and Applications*. SCITEPRESS - Science and Technology Publications, (2023).
- [22] Kira Maag, Matthias Rottmann, and Hanno Gottschalk, ‘Time-dynamic estimates of the reliability of deep semantic segmentation networks’, in *IEEE International Conference on Tools with Artificial Intelligence (ICTAI)*, (2020).
- [23] Aleksander Madry, Aleksandar Makelov, Ludwig Schmidt, Dimitris Tsipras, and Adrian Vladu, ‘Towards deep learning models resistant to adversarial attacks’, in *International Conference on Learning Representations (ICLR)*, (2018).
- [24] Dongyu Meng and Hao Chen, ‘Magnet: A two-pronged defense against adversarial examples’, in *ACM SIGSAC Conference on Computer and Communications Security*, (2017).
- [25] Jan Hendrik Metzen, Mummadri Chaithanya Kumar, Thomas Brox, and Volker Fischer, ‘Universal adversarial perturbations against semantic image segmentation’, in *IEEE International Conference on Computer Vision (ICCV)*, (2017).
- [26] Andy Michel and Rickard Ewetz, ‘Gradient-based adversarial attack detection via deep feature extraction’, in *SoutheastCon*, (2022).
- [27] Seyed-Mohsen Moosavi-Dezfooli, Alhussein Fawzi, and Pascal Frossard, ‘Deepfool: A simple and accurate method to fool deep neural networks’, in *IEEE/CVF Conference on Computer Vision and Pattern Recognition (CVPR)*, (2016).
- [28] Krishna Kanth Nakka and Mathieu Salzmann, ‘Indirect local attacks for context-aware semantic segmentation networks’, in *European Conference on Computer Vision (ECCV)*, (2020).
- [29] Federico Nesti, Giulio Rossolini, Saasha Nair, Alessandro Biondi, and Giorgio C. Buttazzo, ‘Evaluating the robustness of semantic segmentation for autonomous driving against real-world adversarial patch attacks’, in *IEEE/CVF Winter Conference on Applications of Computer Vision (WACV)*, (2022).
- [30] Huihui Pan, Yuanduo Hong, Weichao Sun, and Yisong Jia, ‘Deep dual-resolution networks for real-time and accurate semantic segmentation of traffic scenes’, *IEEE Transactions on Intelligent Transportation Systems*, (2022).
- [31] Jérôme Rony, Jean-Christophe Pesquet, and Ismail Ben Ayed. Proximal splitting adversarial attacks for semantic segmentation, 2022.
- [32] Peter J. Rousseeuw and Katrien Van Driesssen, ‘A fast algorithm for the minimum covariance determinant estimator’, *Technometrics*, (1999).
- [33] Bernhard Schölkopf, Robert C Williamson, Alex Smola, John Shawe-Taylor, and John Platt, ‘Support vector method for novelty detection’, in *Advances in Neural Information Processing Systems*. MIT Press, (1999).

- [34] Robert Tibshirani, ‘Regression shrinkage and selection via the lasso’, *Journal of the Royal Statistical Society: Series B*, (1996).
- [35] Jingdong Wang, Ke Sun, Tianheng Cheng, Borui Jiang, Chaorui Deng, Yang Zhao, Dong Liu, Yadong Mu, Mingkui Tan, Xinggang Wang, Wenyu Liu, and Bin Xiao, ‘Deep high-resolution representation learning for visual recognition’, *IEEE Transactions on Pattern Analysis and Machine Intelligence*, (2021).
- [36] Prameesha S. Weerasinghe, Sarah M. Erfani, Tansu Alpcan, Christopher Leckie, and Margreta Kuijper, ‘Unsupervised adversarial anomaly detection using one-class support vector machines’, *International Symposium on Mathematical Theory of Networks and Systems*, (2018).
- [37] Chaowei Xiao, Ruizhi Deng, Bo Li, Fisher Yu, Mingyan Liu, and Dawn Song, ‘Characterizing adversarial examples based on spatial consistency information for semantic segmentation’, in *European Conference on Computer Vision (ECCV)*, (2018).
- [38] Cihang Xie, Jianyu Wang, Zhishuai Zhang, Yuyin Zhou, Lingxi Xie, and Alan Loddon Yuille, ‘Adversarial examples for semantic segmentation and object detection’, *IEEE International Conference on Computer Vision (ICCV)*, (2017).
- [39] Xiaogang Xu, Hengshuang Zhao, and Jiaya Jia, ‘Dynamic divide-and-conquer adversarial training for robust semantic segmentation’, in *IEEE International Conference on Computer Vision (ICCV)*, (2021).
- [40] Maksym Yatsura, Kaspar Sakmann, N. Grace Hua, Matthias Hein, and Jan Hendrik Metzen. Certified defences against adversarial patch attacks on semantic segmentation, 2022.
- [41] Changqian Yu, Jingbo Wang, Chao Peng, Changxin Gao, Gang Yu, and Nong Sang, ‘Bisenet: Bilateral segmentation network for real-time semantic segmentation’, in *European Conference on Computer Vision*, (2018).
- [42] Qifei Zhou, Rong Zhang, Bo Wu, Weiping Li, and Tong Mo, ‘Detection by attack: Detecting adversarial samples by undercover attack’, in *European Symposium on Research in Computer Security (ESORICS)*, (2020).

## APPENDIX

### A More Adversarial Examples

In this section, we provide qualitative results for the considered attacks. In Figure 6 and Figure 7 semantic segmentation predictions for an example image from the Cityscapes dataset are shown and in Figure 8 for an example image from the VOC dataset. For Cityscapes, we observe more pixel changes for the FGSM attack for increasing noise. For the untargeted I-FGSM attack, the predictions result in less different classes across datasets and network architectures. In general, for the weaker HRNet in comparison to the DeepLabv3+, the perturbations are more visible. Even the non-iterative FGSM attacks and also the patch attack show great success.

In Figure 9, Figure 10, and Figure 11, the corresponding entropy heatmaps for the clean images and the perturbed ones are given. The heatmaps for the targeted and untargeted FGSM attack still look similar to the heatmap for the clean image. These attacks change the prediction though, however, shapes are still recognizable. High uncertainties can also be seen in the areas where the attack was successful. For the iterative untargeted FGSM attack, the heatmaps are dark with only high values on the segment boundaries. In this case, the perturbation can be detected as the average uncertainty per image deviates downward from the clean prediction. The iterative targeted attack shows the highest uncertainty, since the predictions consist of comparatively large numbers of different segments and classes. Similar to the clean image, the SSMM and DNNM attacks indicate higher uncertainties in the background while the certainty in the prediction of the road and the cars is high. The patch attack has different effects on both networks, i.e. for the DeepLabv3+, is uncertainty higher in general and especially at the patch boundaries and for the HRNet, the impact on the prediction is stronger, which is also reflected in the heatmaps.

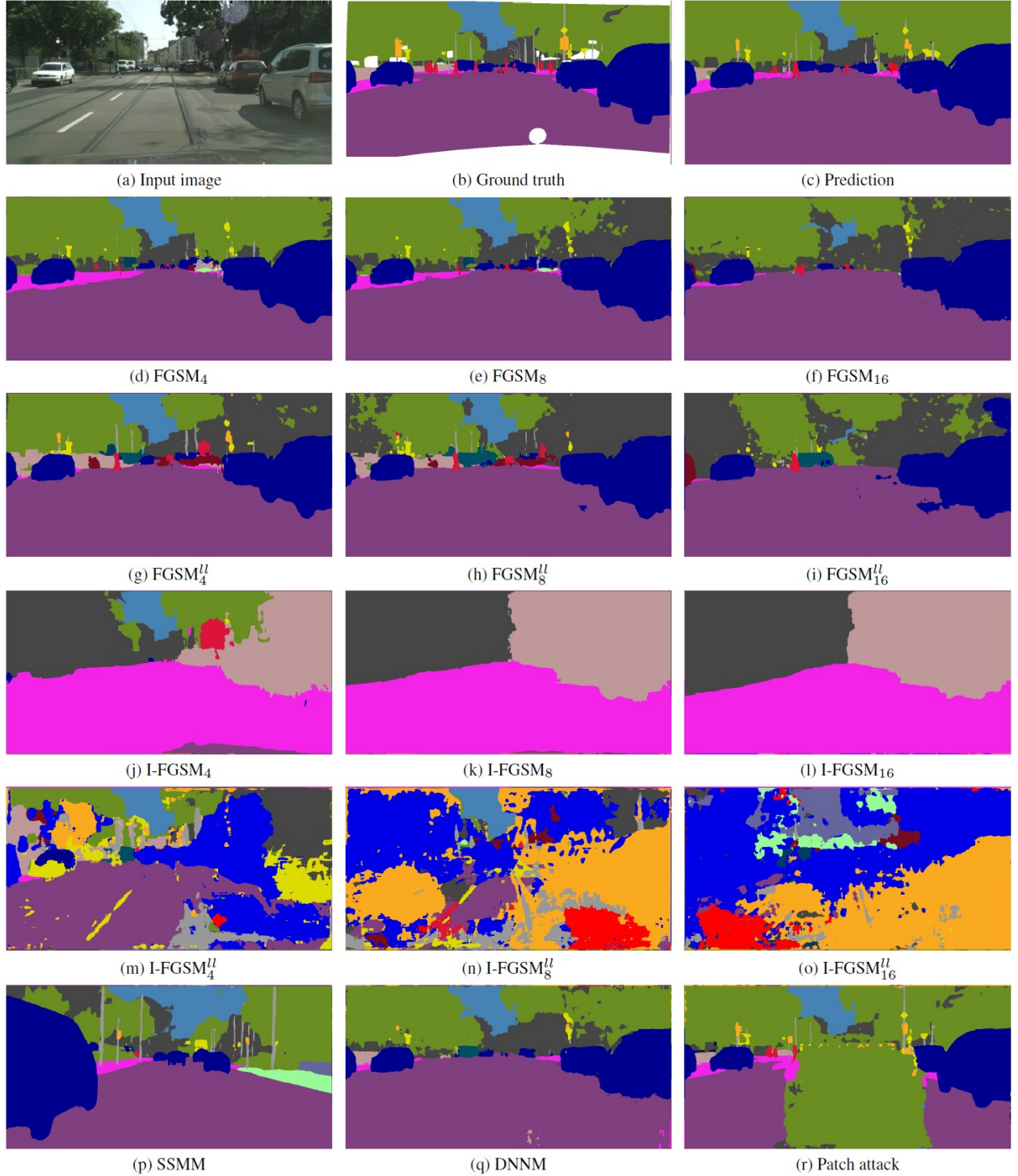


**Figure 6:** Input image (a) with corresponding ground truth (b) for the Cityscapes dataset. Semantic segmentation prediction obtained by the DeepLabv3+ network for a clean image (c) and perturbed images generated by various attacks (d)-(r).

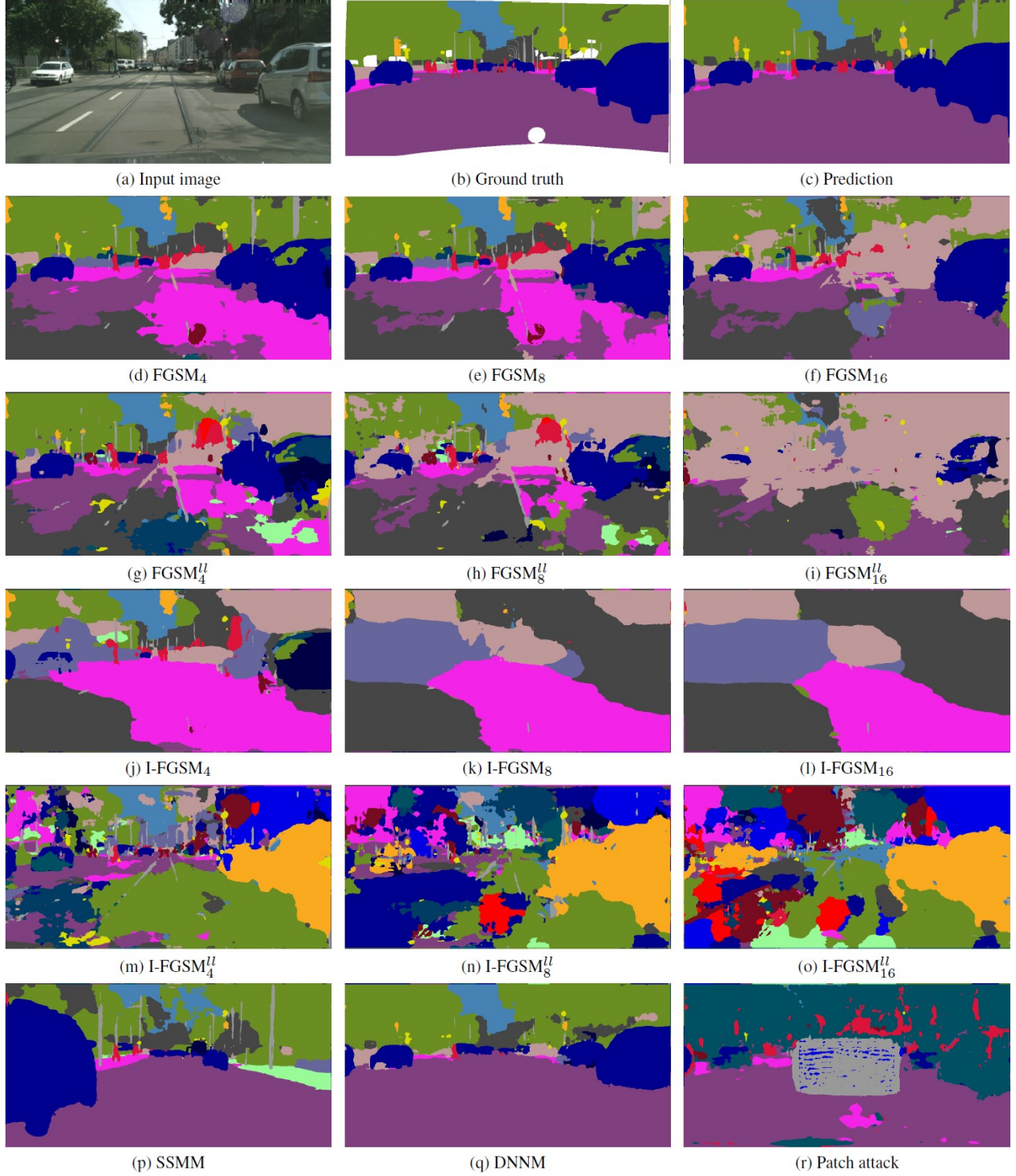


**Figure 7:** Input image (a) with corresponding ground truth (b) for the Cityscapes dataset. Semantic segmentation prediction obtained by the HRNet network for a clean image (c) and perturbed images generated by various attacks (d)-(r).

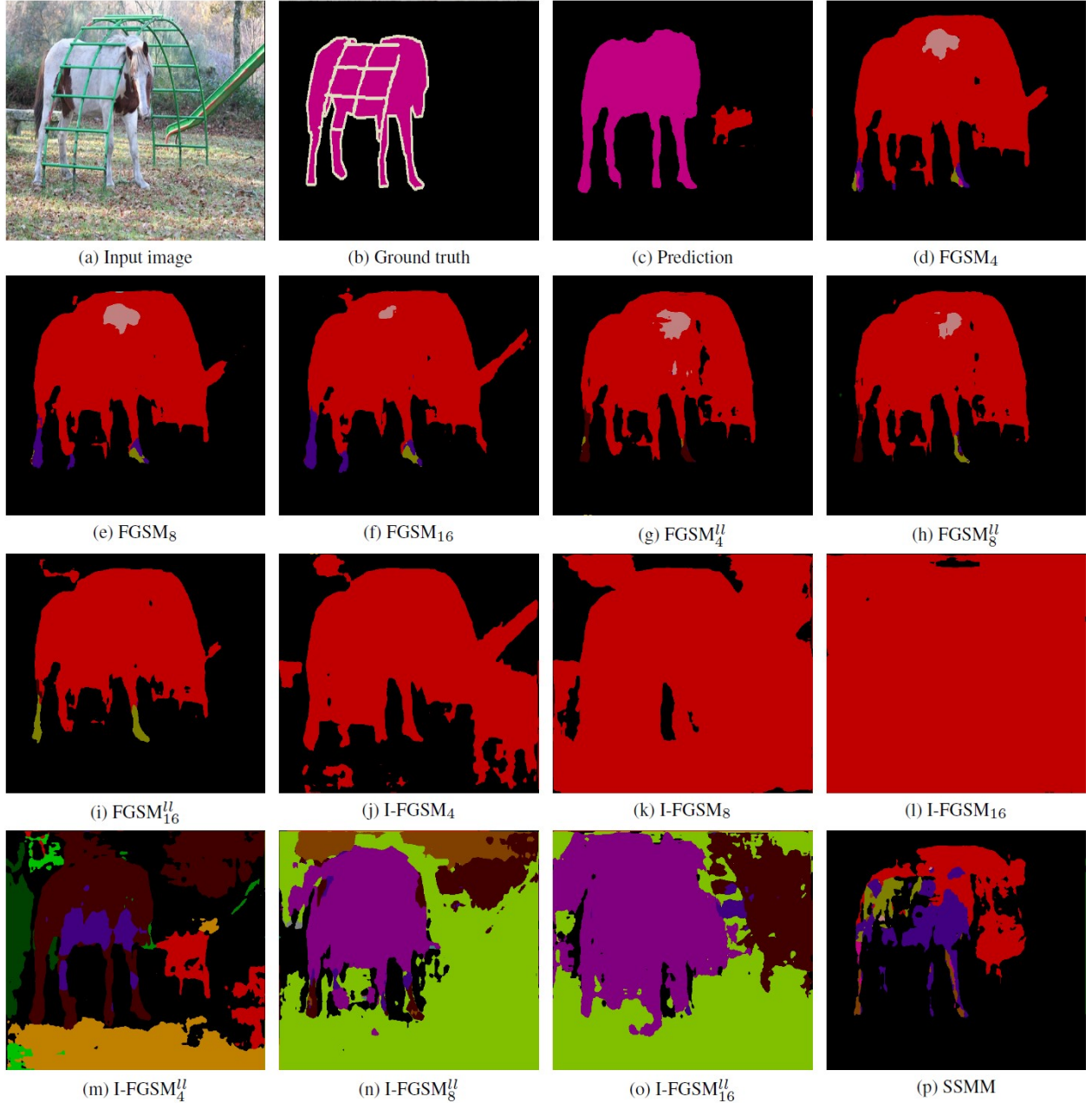


**Figure 8:** Input image (a) with corresponding ground truth (b) for the VOC dataset. Semantic segmentation prediction obtained by the DeepLabv3+ network for a clean image (c) and perturbed images generated by various attacks (d)-(p).

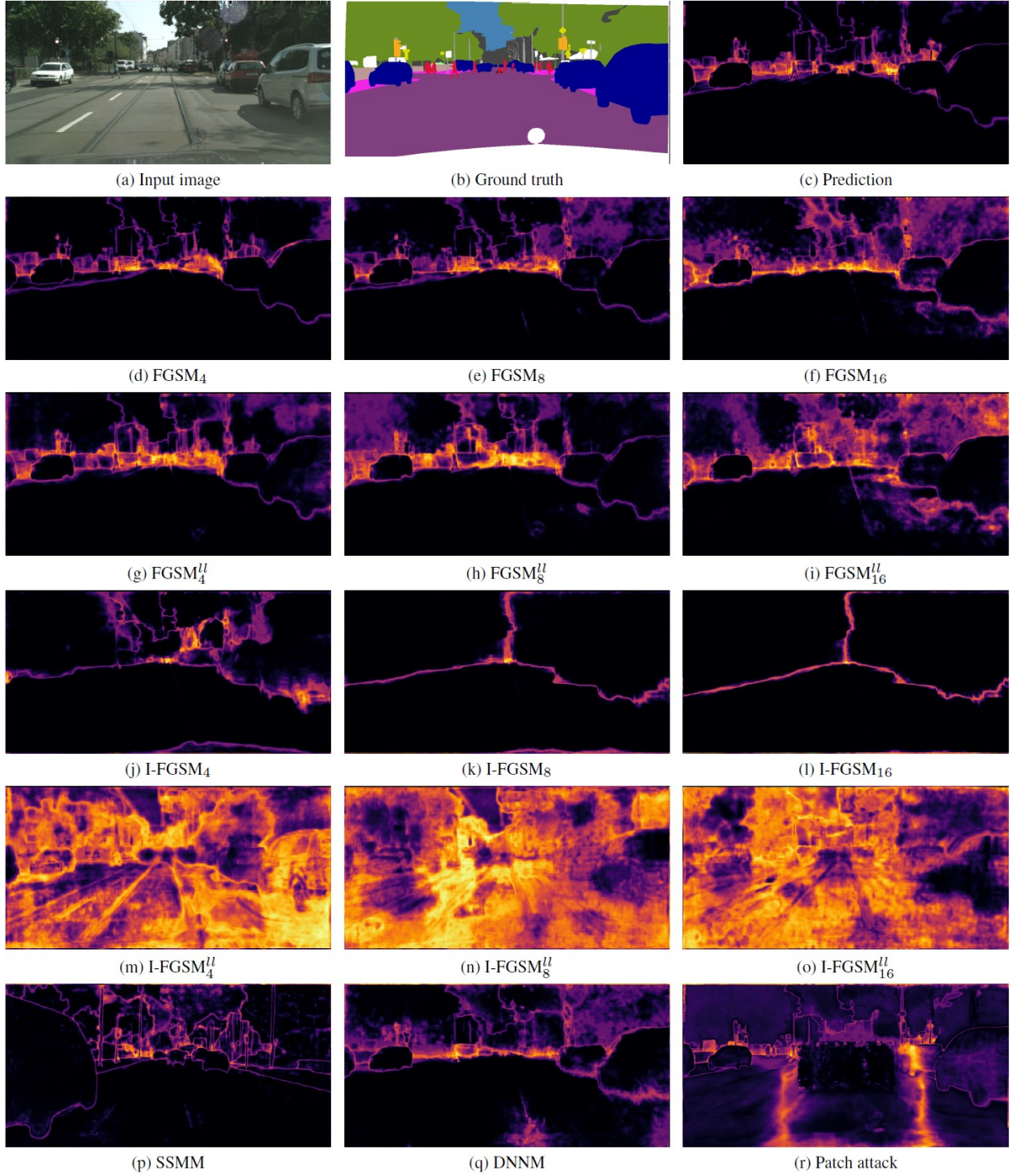


**Figure 9:** Input image (a) with corresponding ground truth (b) for the Cityscapes dataset. Entropy heatmaps obtained by the DeepLabv3+ network for a clean image (c) and perturbed images generated by various attacks (d)-(r).

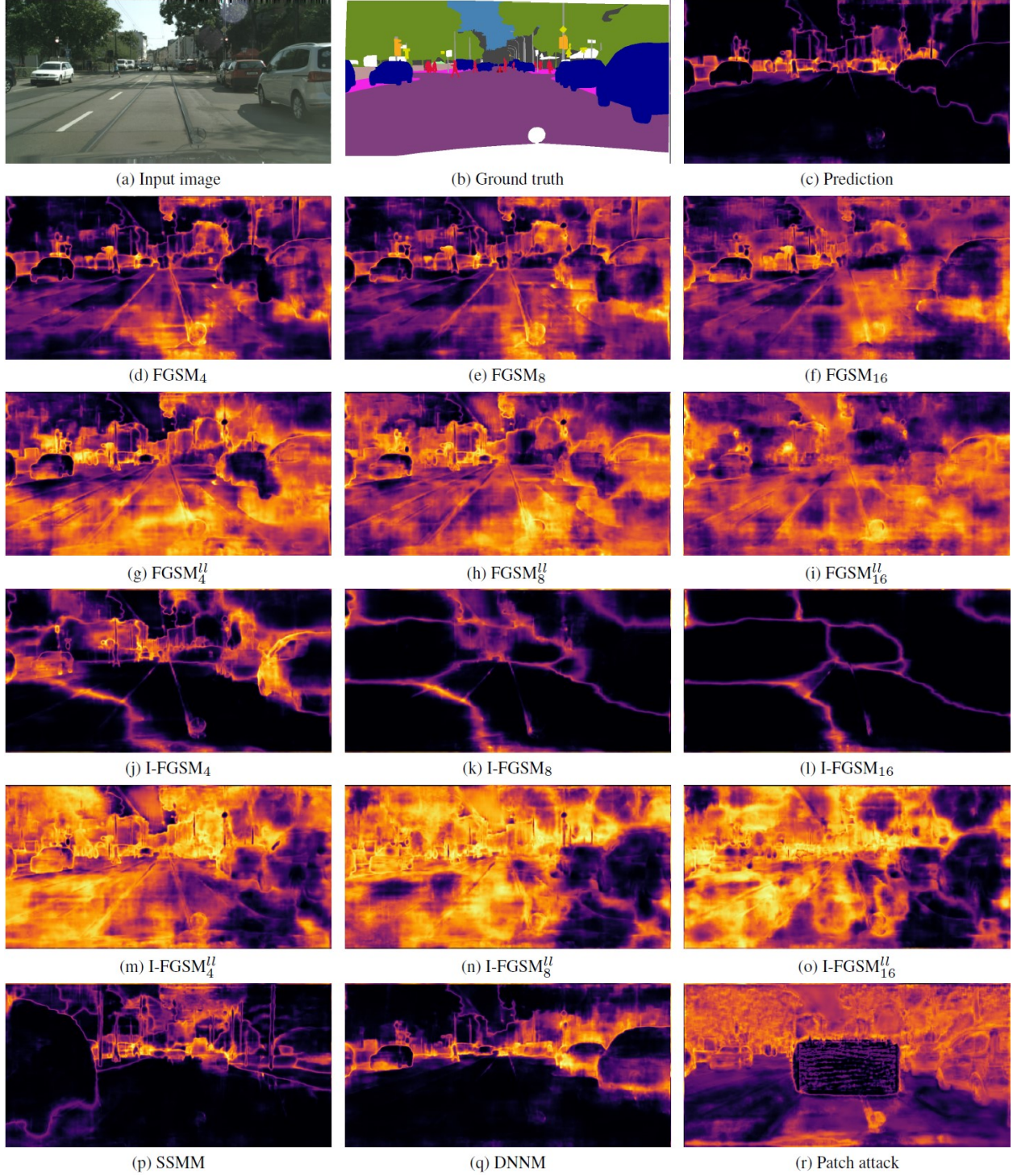


**Figure 10:** Input image (a) with corresponding ground truth (b) for the Cityscapes dataset. Entropy heatmaps obtained by the HRNet network for a clean image (c) and perturbed images generated by various attacks (d)-(r).

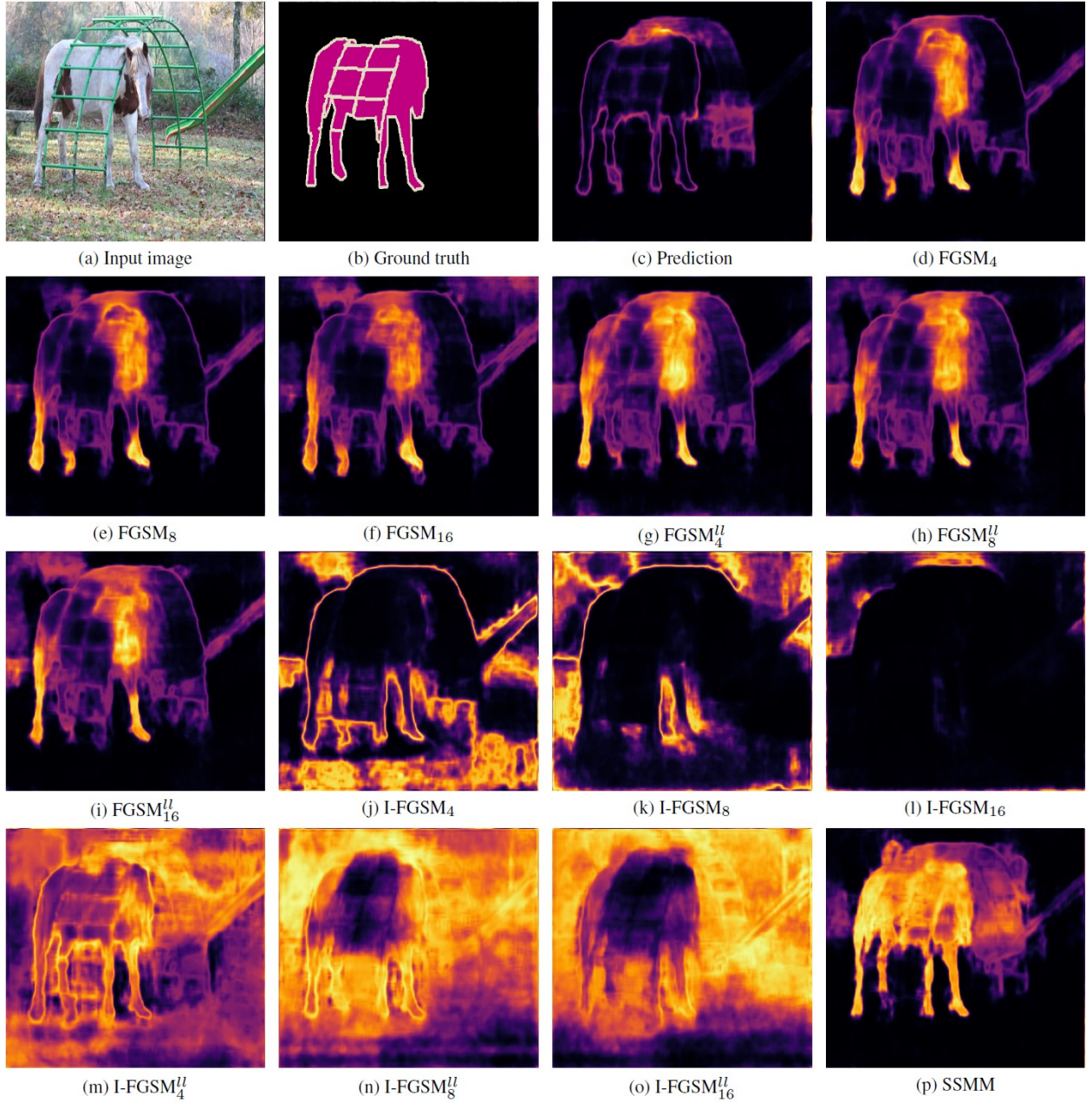


**Figure 11:** Input image (a) with corresponding ground truth (b) for the VOC dataset. Entropy heatmaps obtained by the DeepLabv3+ network for a clean image (c) and perturbed images generated by various attacks (d)-(p).